Results From The Milagro All-Sky TeV Gamma-Ray Observatory

Gus Sinnis (for the Milagro collaboration)
Los Alamos National Laboratory, Los Alamos, NM 87545, USA

Abstract

Milagro is a water Cherenkov telescope sensitive to gamma rays with energies above 100 GeV. Unlike air-Cherenkov telescopes, Milagro continuously views the entire overhead sky. This capability makes it well suited to search for transient phenomena such as gamma-ray bursts and to discover new phenomena. Using a new technique to reject the cosmic-ray background Milagro has surveyed the entire Northern hemisphere for TeV gamma-ray sources. Over the period from December 2000 through December 2001 Milagro has detected the Crab Nebula and the active galaxy Mrk421. No other point sources have been detected over this time period. There is also a preliminary detection of the galactic plane.

1. Introduction

High-energy gamma-ray astronomy is a relatively new field of astronomical exploration. When viewed in TeV gamma rays the universe appears quite different than when viewed optically. The sources of TeV photons are typically non-thermal and contain highly relativistic particles. These sources tend to be episodic or transient in nature. Therefore there is a strong incentive to build an instrument capable of continuously monitoring a large region of the sky in this energy range. Milagro is the the most sensitive all-sky detector operating at TeV energies and has a proven capability to reject the cosmic ray background. Using this background rejection method we have detected emission from the Crab nebula, Mrk421, and possibly from the from the galactic plane. A search of the entire Northern hemisphere has been performed and the results are presented here.

2. The Milagro Detector

The central detector of Milagro is a 264-million liter water reservoir, located 35 miles west of Los Alamos, NM at an altitude of 2650 m asl (750 g/cm^2). The reservoir measures 80m×60m×8m deep and is covered with a light-tight cover. The reservoir is instrumented with 753 photomultiplier tubes (PMTs) de-

pp. 1–7

ployed in two layers. The top layer of 450 PMTs is submerged under 1.5 meters of water and set on a 2.8m×2.8 m grid. The bottom layer of PMTs is under 6 meters of water and also set on a 2.8m×2.8 m grid. The top layer of PMTs is used to reconstruct the direction of the air shower and the bottom layer is used to measure the penetrating component of the air showers and thereby reject the cosmic-ray background. A complete description of a prototype instrument, Milagrito, is given in Atkins *et al.* 2000.

The trigger rate in Milagro is roughly 1700 Hz with a data throughput of 5 MBytes/sec. There are insufficient resources available to save all of this data to tape. Therefore the events are reconstructed in real time by a computer farm. The reconstructed information from each event (core position, arrival direction, event time, information used to determine the composition of the primary particle, etc.) is saved to disk and backed up to tape. In addition, the raw data is saved for events near preselected objects of interest (the Crab, the Sun and Moon, etc.). In the advent of GRB within the field-of-view of Milagro all of the raw data within one hour of the burst is saved. Roughly 100 GBytes of data per day of tape is written.

3. Background Rejection in Milagro

The hadronic background from cosmic rays can outnumber the gamma rays by a factor of 1000 to 1 (or more depending upon the angular size of the region examined). The Whipple collaboration has perfected the imaging technique for differentiating between hadronic cosmic rays and gamma ray induced air showers in an atmospheric Cherenkov telescope(Hillas 1985 and Weeks 1977). In the past year we have developed a technique that uses the information in the bottom layer of Milagro to reject the hadronic background. Hadronic cosmic rays generate air showers that contain penetrating particles, muons, hadrons that shower in the water, or very energetic electromagnetic particles. Such penetrating particles will deposit a large amount of light in a small region in the bottom of the detector. An air shower that contains no penetrating particles will illuminate the bottom of the detector with a relatively uniform, low level of light. Small clumps of high light levels are easily distinguished in the proton induced events. We have found a simple parameter, known as compactness (C=NPMT(>2PE)/PeMax - over the bottom layer), that is sensitive to the differences between proton and gamma ray induced events. The numerator is the number of PMTs in the bottom layer that are struck with more than 2 photoelectrons (PEs) and the denominator is the pulse height, in PEs, of the brightest PMT in the bottom layer. Penetrating particles, that illuminate a small region on the bottom lead to small values of C, while

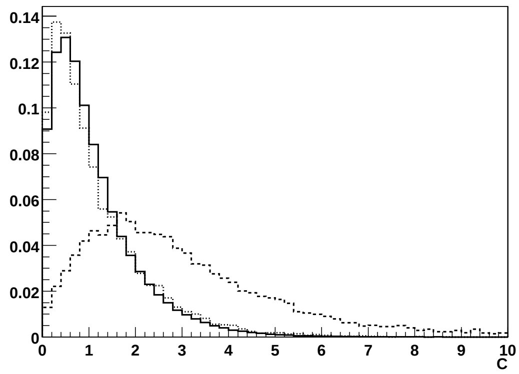

Fig. 1. The compactness distribution of Monte Carlo proton event (solid line), Monte Carlo gamma ray events (dashed line) and data (dotted line).

gamma ray events lead to large values of C. Figure 1 shows the C distribution for proton and gamma ray induced events (from simulations) and data. There is good agreement between data and simulations of proton induced events. By rejecting all events with $C < 2.5$ we remove 90% of the background events while retaining 50% of the gamma ray induced events: an improvement in sensitivity (Q value) of 1.6.

4. The Crab Nebula

We have analyzed two years of data from the Crab. Since all of the raw data within 8 degrees in declination of the Crab is saved we have the luxury of reanalyzing old data with the recently developed background rejection capabilities. Thus this dataset is different from that used below, where the entire sky is searched for gamma-ray sources. The dataset begins on June 8, 1999 and ends on April 1, 2002. Because of detector down time the effective exposure during this time interval is 839 days. The results of the Crab analysis (with and without the compactness cut) are given in Table 1. While the C cut removed 89% of the data, in agreement with the Monte Carlo simulations, the efficiency for gamma rays appears to be greater than 1. This nonphysical result arises from the large fluctuations in the background level and is consistent with expectations at the 5% level..

The observed signal can be used to estimate the flux of TeV gamma rays from the Crab nebula. However, since the energy resolution of Milagro is relatively poor it is not meaningful to fit the shape of the spectrum. Instead three different functions have been assumed for the spectral shape and the differential

Table 1. Results of the analysis of data from the Crab Nebula. The results are given for all data and for data that passes the compactness criteria

Data Selection	ON Source	Background	Excess	Significance
All Data	17,922,478	17,915,678	6800	1.5σ
C > 2.5	2,291,429	2,282,021	8108	6.0σ

Table 2. Flux measurement from Milagro under three different assumptions for the source spectrum. The top line contains the measurement from Milagro. For comparison we give the measurements from the references in the bottom line. The spectral shapes (S_1, S_2, and S_3 are described in the text. I_0 is given in units of $10^{-7}m^{-2}s^{-1}TeV^{-1}$.

	S_1	S_2	S_3
I_0	$2.07 \pm 0.38^{stat} \pm 1.2^{sys}$	$2.39 \pm 0.44^{stat} \pm 1.4^{sys}$	$2.3 \pm 0.42^{stat} \pm 1.4^{sys}$
I_0	$3.20 \pm 0.17^{stat} \pm 0.6^{sys}$	$3.25 \pm 0.14^{stat} \pm 0.6^{sys}$	$2.79 \pm 0.022^{stat} \pm 0.5^{sys}$

flux coefficient is determined for each of these. The three spectral functions are: $dN/dE = E^{-2.49}$ (Hillas et al. 1998) (S_1 in Table 2), $dN/dE = E^{-2.44-0.151\lg(E)}$ (Hillas et al.1998) (S_2 in Table 2), and $dN/dE = E^{-2.59}$ (Aharonian et al. 2000) (S_3 in Table 2). Since the response of Milagro is dependent upon zenith angle Monte Carlo simulations are used to estimate the effective area of Milagro as a function of energy, averaged over a transit of the Crab. For a source with spectrum of $f(E)$ the double integral over energy and time,

$$I_0 \int \int A_\gamma(E, \theta(t)) f(E) dEdt events/day \tag{1}$$

is evaluated for the three spectral functions $f(E)$. In the above integral A_γ is the effective area for gamma rays with energy E arriving from a zenith angle θ. The calculation of the effective area includes the effect of the background rejection criteria ($C > 2.5$), the angular reconstruction, and the trigger requirement of the detector (number of PMTs in the top layer > 60). After determining the value of the integrand, the observed excess (9.3 events/day) is used to determine I_0. The results for the three different spectral shapes are given in Table 2. While the Milagro data seems to favor the steeper spectra at higher energies the systematic errors are too large to draw a definitive conclusion.

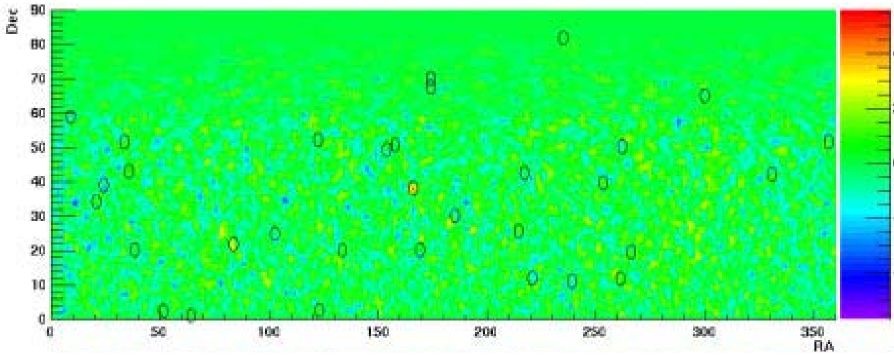

Fig. 2. The northern hemisphere as seen in TeV gamma rays by Milagro. The circles mark the locations of the 26 AGN selected by Costamante and Ghisellini 2002 along with the known sources of TeV gamma rays.

5. Survey of the Northern Sky

The above analysis has been applied to the northern hemisphere. In this case the data set begins on December 15, 2000 and ends on December 15, 2001. The beginning date marks the date when the online (real-time) reconstruction algorithms incorporated the background rejection method described above and an improved core fitting algorithm. Figure 2 shows a map of the Northern Hemisphere in galactic coordinates. The brightest object in the sky during this time period was Mrk421 (near the center of Figure 2). Between January 2000 and May 2001 the emission from Mrk421 was roughly 1.5 times that of the Crab in Milagro. After this the emission apparently fell below the sensitivity of Milagro and then in July of 2001 seems to have been emitting at a level of roughly 0.75 times the Crab. However, the statistical significance of the measurement during the latter time period is marginal ($\sim 2.5\sigma$).

6. TeV Gamma Ray Emission from the Galactic Plane

Cosmic ray interactions with matter in the galaxy will give rise to the production of gamma rays. To date the highest energy measurement of this diffuse emission from the galaxy has been made by EGRET. While one might expect the spectrum of the diffuse gamma rays to match the cosmic ray spectrum EGRET measures a significantly harder spectrum ($E^{-2.3}$). The expected signal to background ratio is of the order 10^{-4}. With such a low signal level systematic errors in the analysis must be a prime concern. A new analysis technique was developed to search for such a weak, diffuse signal in the Milagro dataset. The details of

Table 3. Results of a search for TeV emission from the galactic plane.

	Inner Galaxy	Inner Galaxy	Outer Galaxy	Outer Galaxy
Thickness	$\pm 2°$	$\pm 5°$	$\pm 2°$	$\pm 5°$
Excess	$17,800$	$36,460$	$-4,086$	$-13,979$
Bkgnd	4.35×10^7	1.08×10^8	4.64×10^7	1.15×10^8
$F_\gamma/F_{cr} \times 10^{-5}$	$11.2 \pm 4.1(2.7\sigma)$	$9.4 \pm 2.7(3.5\sigma)$	<9.7	<7.1

this technique are beyond the scope of this paper and can be found in Fleysher 2002. Milagro's exposure to the galactic plane is limited by the latitude of the experiment and the galactic center is not visible. Using the EGRET measurements as a guide the galaxy was divided into two portions: the inner galaxy, spanning galactic longitude from 20 to 100 degrees and the outer galaxy spanning galactic longitudes from 140 degrees to 220 degrees. In addition two different possible disk thicknesses were examined: $\pm 2°$ and $\pm 5°$ around the galactic plane. Only data that passed the background rejection cut given above have been analyzed. The analyzed data set spans 14 months from December 2000 to February 2001. The results of the analysis are given in Table 3. The region of the inner galaxy yields a signal of limited statistical significance. The results should improve as more data is analyzed. The measurements given are preliminary and are currently under further study. If the above signal is indeed due to a diffuse flux of TeV gamma rays in the galactic plane it would be the highest energy measurement made to date of this source. To compare the result to EGRET measurements one must account for the different exposures (in galactic latitude and longitude) of the two instruments. This work is still in progress.

7. References

1. Aharonian, F.A., *et al.* 2000, ApJ, 539,317
2. Atkins, R., *et al.* 2000, NIM A 449, 478
3. Fleysher, R. 2002, PhD Thesis, New York University
4. Hillas, A.M. 1985, Proc. of 19th ICRC (La Jolla), 3, 445
5. Hillas, A.M., *et al.* 1998, Astrophys J., 503, 744
6. Weekes, T.C. and Turver, K.E. 1977, Proc. of 12th Eslab Symposium, eds. R.D. Wills and B. Battrick, 279